IOPscience iopscience.iop.org

Home Search Collections Journals About Contact us My IOPscience

Ferroelectricity and negative temperature coefficient of resistance in pulsed-laser-deposited $(Pb,Sr)TiO_3$ films

This content has been downloaded from IOPscience. Please scroll down to see the full text.

2008 J. Phys. D: Appl. Phys. 41 085304

(http://iopscience.iop.org/0022-3727/41/8/085304)

View the table of contents for this issue, or go to the journal homepage for more

Download details:

IP Address: 140.113.38.11
This content was downloaded on 25/04/2014 at 16:22

Please note that terms and conditions apply.

IOP PUBLISHING JOURNAL OF PHYSICS D: APPLIED PHYSICS

J. Phys. D: Appl. Phys. **41** (2008) 085304 (7pp) doi:10.1088/0022-3727/41/8/085304

Ferroelectricity and negative temperature coefficient of resistance in pulsed-laser-deposited (Pb,Sr)TiO_3 films

Jyh-Liang Wang[1], Yi-Sheng Lai[2], Sz-Chian Liou[3], Chun-Chien Tsai[1], Bi-Shiou Chiou[1] and Huang-Chung Cheng[1]

[1] Department of Electronics Engineering and Institute of Electronics, National Chiao Tung University, 1001 Ta Hsueh Rd., Hsinchu 30010, Taiwan, Republic of China
[2] Department of Materials Science and Engineering, National United University, Miaoli 36003, Taiwan, Republic of China
[3] Center for Condensed Matter Sciences, National Taiwan University, Taipei 10617, Taiwan, Republic of China

E-mail: yslai@nuu.edu.tw

Received 17 September 2007, in final form 25 February 2008
Published 14 March 2008
Online at stacks.iop.org/JPhysD/41/085304

Abstract

(Pb,Sr)TiO_3 films deposited on Pt/SiO_2/Si substrates by pulsed-laser deposition (PLD) at 400 °C with oxygen pressures ranging from 50 to 200 mTorr have been investigated. The paraelectricity-to-ferroelectricity transition of films depends on the oxygen pressure during deposition. Films deposited at 200 mTorr exhibit paraelectric-like nature, whereas films deposited at lower pressures present the ferroelectric characteristic. The (Pb,Sr)TiO_3 film is found to exhibit a negative temperature coefficient of resistance (NTCR) at the measurement temperature ranging from 30 to 390 °C. This work demonstrates that the ferroelectricity/paraelectricity and the temperature coefficient of resistance of (Pb,Sr)TiO_3 films could be controlled by oxygen pressures during PLD.

(Some figures in this article are in colour only in the electronic version)

1. Introduction

Ferroelectric semiconducting materials, with a perovskite structure, have attracted much attention lately due to their potential applications in thermistor sensors [1–8]. Among these materials, (Pb,Sr)TiO_3 (PSrT) have attracted considerable interest in the composite effect of negative and positive temperature coefficient of resistance (TCR) (NTCR and PTCR), first demonstrated by Hamata *et al* in 1988 [1]. In addition, PSrT has a relatively low sintering temperature compared with the conventional barium titanate [2]. PSrT ceramics usually exhibit an NTCR behaviour below Curie temperature (T_c) and a PTCR effect above T_c [1–6]. Moreover, a PSrT solid solution is constituted of $SrTiO_3$ (STO) and $PbTiO_3$ (PTO). The T_c of PSrT can be linearly adjusted from −220 to 490 °C by varying the lead (Pb) content [9, 10]. It is established that Pb substituted by strontium (Sr) in the PTO film will decrease the crystallization temperature at room temperature [11,12]. The TCR effect of the PSrT bulk prepared by conventional ceramic solid state sintering processes has been reported [2–6]. However, there is a lack of sufficient studies on the TCR properties of PSrT films, which can be used as film-type thermistor sensors embedded into micro-electro-mechanical systems (MEMS). As a consequence, the subject needs further investigations on the film characteristics.

In this work, the (Pb,Sr)TiO_3 films are prepared at low temperature (400 °C) by the pulsed-laser deposition (PLD) technique, which is simple, versatile, capable of growing a wide variety of stoichiometric oxide films without subsequent high temperature annealing and excellent for fabricating thin films with complex compounds. Hence, PLD is a potential technique, which could be integrated into the low-temperature semiconductor process to protect the formerly fabricated structure from damage and eliminate the volatilization of PbO in lead-titanate-based thin films [13, 14]. In general, the structural and electrical characteristics of the PLD ferroelectric

 © 2008 IOP Publishing Ltd Printed in the UK

films are strongly affected by process parameters, such as oxygen pressure. Several papers have reported the effect of oxygen pressure on the characteristics of PLD ferroelectric films [15–18]. However, the properties of PLD PSrT films prepared on the Pt/SiO_2 substrate are not much addressed [19–21]. Hence, this work is focused on the effects of oxygen pressure on the structural and electrical characteristics of Pt/PSrT/Pt capacitors prepared by low-temperature PLD. Moreover, the TCR characteristics of the PLD PSrT films are also investigated.

2. Experimental

Thin PSrT films 200 nm thick were deposited on the $Pt/SiO_2/Si$ substrate with a KrF PLD system (Lambda Physik Excimer Laser LPX 210i, $\lambda = 248$ nm). A set of optical lens was used to focus the excimer laser beam onto the stoichiometric $(Pb_{0.6}Sr_{0.4})TiO_3$ target in vacuum. The vacuum chamber was pumped down to a base pressure of 0.1 mTorr and then oxygen (O_2) was refilled as the working gas. The ablated species of the target were transferred and deposited on the substrate heated by a thermal heater. The target to substrate distance was 4 cm. The deposition temperature was fixed at a relatively low substrate temperature of 400 °C, calibrated at the wafer upper surface. The oxygen pressure was used as a variable from 50 to 200 mTorr. The laser pulsed rate and the average energy fluence were 5 Hz and 1.55 J pulse^{-1} cm^{-2}, respectively.

The surface morphology of PSrT films was examined by field emission scanning electron microscopy (FESEM) (S-4000, Hitachi Co.). The composition of the PSrT films was characterized by Auger electron spectroscopy ((AES) Auger 670 PHI Xi, Physical Electronics). Plan-view and cross-sectional transmission electron microscopy (TEM) samples were prepared by standard sample preparation techniques with tripod polishing and ion milling using the Gatan precision ion polishing system (PIPS) system operated at 3 kV. The TEM experiments were carried out on a JEM-2000FX (JEOL Ltd) operated at 200 keV.

Patterned Pt top electrodes, with a thickness of 100 nm and a diameter of 75 μm, were deposited by the sputtering process to form a Pt/PSrT/Pt capacitor structure for electrical measurements. An automatic measurement system that combines an IBM computer, a semiconductor parameter analyzer (4156C, Agilent Technologies) and a probe station with an embedded heater was used to measure the current–voltage (I–V) characteristics as a function of the measurement temperature (T_m) ranging from 30 to 390 °C. The TCR values were evaluated from the temperature dependent current data. The ferroelectric polarization versus electric field (P–E) characteristics of the PSrT film were determined directly by virtual ground circuits (RT-66A standardized ferroelectric testing system, Radiant Technologies).

3. Results and discussion

Figures 1(a)–(c) show polarization versus electric field plots of PSrT films deposited at various oxygen pressures. It is found that hysteresis loops only appear for films deposited at 50 and 100 mTorr, but figure 1(c) shows the linear characteristic for films deposited at 200 mTorr. The hysteresis loops are larger for films deposited at 100 mTorr than those deposited at 50 mTorr. To realize the dependence of polarization on the oxygen pressure, we examine the microstructure of PSrT films. The connection between polarization and microstructure is discussed below.

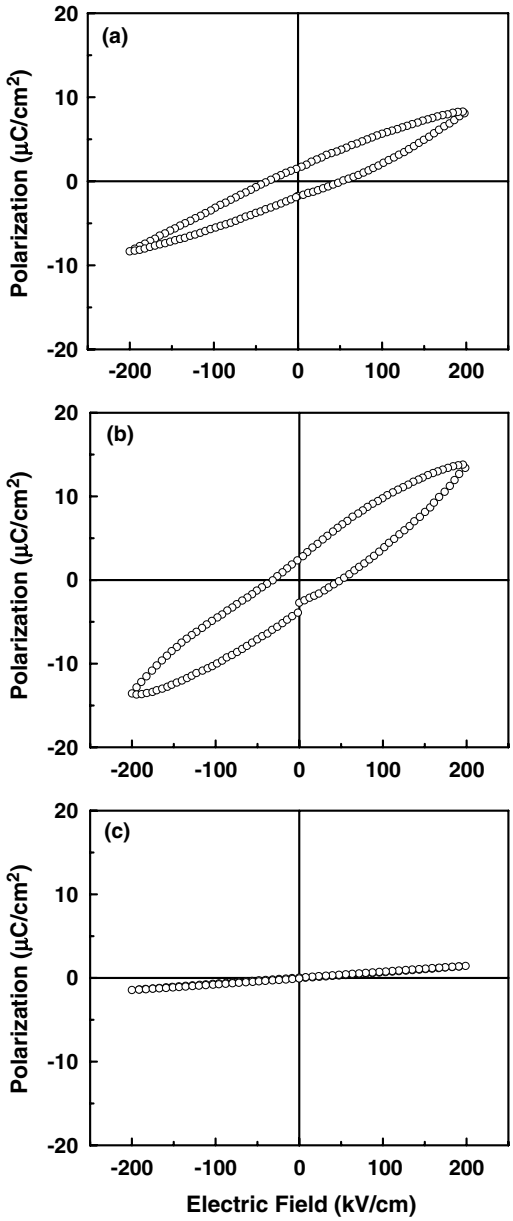

Figure 1. Polarization–electric field (P–E) hysteresis loops of Pt/PSrT/Pt capacitors prepared with oxygen pressure at (a) 50 mTorr, (b) 100 mTorr and (c) 200 mTorr.

Figure 2 shows SEM surface morphologies of PLD PSrT films deposited at various oxygen pressures on $Pt/SiO_2/Si$ (1 0 0) wafers. It is seen that the grain size decreases with increasing oxygen pressure, implying that the number of grain boundaries increases as the oxygen pressure increases. The film morphology also becomes denser as the oxygen pressure increases. The TEM images of PSrT films deposited at 50 mTorr and 200 mTorr are shown in figures 3(a) and (b),

respectively. PSrT films deposited at 50 mTorr show a poly-grain structure with an uneven distribution of grain sizes. Furthermore, some regions reveal the amorphous state and can be observed from the electron diffraction patterns with diffused rings (inset of figure 3(*a*)). The images of films deposited at 200 mTorr reveals a denser, more uniform poly-grain distribution 60–80 nm in diameter and less amorphous regions. The polarization is found to be dependent on the tetragonality (c/a) ratio of the lattice (i.e. the ratio of the c-axis to the a-axis lattice constant). c/a is identified by electron diffraction patterns of large-area plan-view TEM samples as shown in the insets of figures 3(*a*) and (*b*). The camera length was calibrated by using Si diffraction patterns, and the lattice spacing (d) was evaluated from the patterns. In addition, the lattice spacing along [0 0 1] and [1 1 0] was also obtained from the HRTEM image by multi-slice simulations (figure 4). It is reported that the atomic positions of heavy metals are correct to within about 10 pm (0.1 Å) if the resolution of the image is 0.25 nm [22]. In our HRTEM experiment, the resolution of the image is 0.1 nm. As a result, the accuracy of sub-0.1 Å could be reliable. The c/a ratios of those PSrT films deposited at 50 mTorr and 200 mTorr are calculated to be ∼1.03 and ∼1.00, respectively, as shown in table 1. The film deposited at 50 mTorr reveals stronger (1 0 0) orientation and a more distinct C–E hysteresis loop than the film deposited at 200 mTorr, showing stronger ferroelectricity. Hence, the cubic structure exhibits paraelectricity, whereas the tetragonal structure exhibits ferroelectricity. As a result, the PSrT film deposited at 50 mTorr shows a tetragonal structure and makes a transition to a cubic-like structure at 200 mTorr. Furthermore, the larger c/a ratio for films deposited at 50 mTorr may be attributed to oxygen deficiency [23, 24]. According to the AES analysis (table 2), it indicates that PSrT films deposited at a higher oxygen pressure have a higher oxygen concentration. Because the ferroelectric dipole originates from ionic displacement in the c-axis direction, large spontaneous polarization is obtained with the elongated c-axis (i.e. large c/a ratio). In other words, the ferroelectric properties of PSrT films are the combined effect of crystal orientation, microstructure and oxygen content. Therefore, the weak (1 0 0) diffraction peak, c/a ratio ∼1 and higher oxygen concentration may account for the paraelectric-like characteristic of PSrT films deposited at 200 mTorr. It suggests that the physical analysis by TEM closely matches the results of polarization measurements. In addition, cross-sectional high-resolution TEM (HRTEM) images of PSrT films deposited at 50 mTorr and 200 mTorr are shown in figures 4(*a*) and (*b*), respectively. Both of them reveal clear lattice images along the PSrT [1 $\bar{1}$ 0] zone axis. Enlarged zones indicated as squares in figures 4(*a*) and (*b*) are calculated by using multi-slice image simulations and good agreement is observed between the calculated and the experimental contrasts with a crystal thickness of 7 nm and a defocus length of −48 nm.

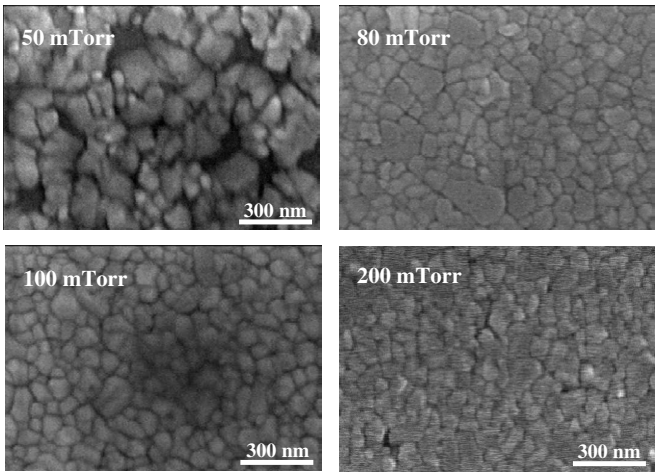

Figure 2. SEM surface morphology of PSrT films deposited at various oxygen pressures on Pt/SiO_2/Si.

Figure 5 shows the dependence of the current density, dc resistance and TCR on the measurement temperature and the biased field, for Pt/PSrT/Pt capacitors prepared at 100 mTorr. The leakage current density increases with increasing T_m (figure 5(*a*)), whereas the resistance decreases with increasing biased fields (figure 5(*b*)), where the symbol at each biased field is extracted from J–E curves. The resistance decreases with T_m (i.e. a negative TCR, NTCR), as exhibited in figure 5(*c*). The TCR can be described as the following equation [7]:

$$\mathrm{TCR} = \frac{1}{R}\left(\frac{\mathrm{d}R}{\mathrm{d}T_m}\right), \tag{1}$$

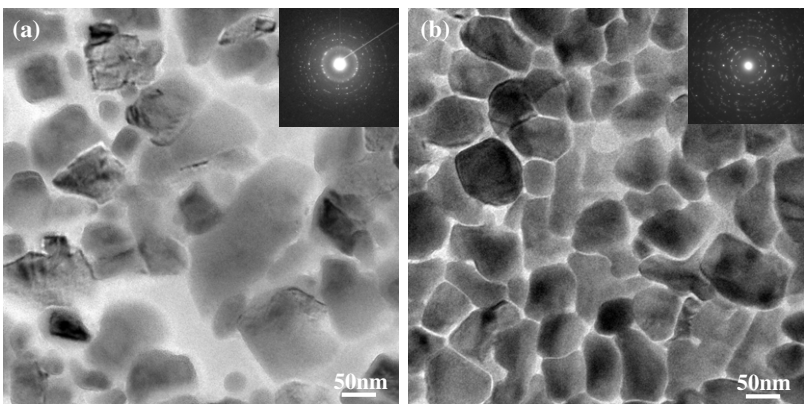

Figure 3. Plane-view TEM images and electron diffraction patterns of PSrT films deposited at (*a*) 50 mTorr and (*b*) 200 mTorr.

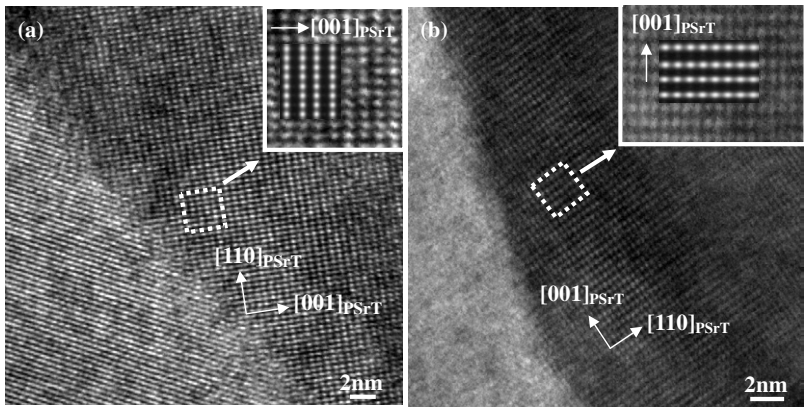

Figure 4. Cross-sectional HRTEM images and multi-slice image simulations for PSrT films deposited at (*a*) 50 mTorr and (*b*) 200 mTorr.

Table 1. The calculation of c/a ratios of PSrT films deposited at 50 and 200 mTorr from diffraction patterns and HRTEM image. The lattice spacing along [0 0 1] and [1 1 0] is simulated by a multi-slice program.

	50 mTorr	200 mTorr
d_{001}	∼4.09 Å	∼4.00 Å
d_{110}	∼2.80 Å	∼2.82 Å
d_{100} (=$d_{110} \times \sqrt{2}$)	∼3.96 Å	∼3.99 Å
c/a ratio	∼1.03	∼1.00

Table 2. Relative element ratio of PLD PSrT films deposited at various oxygen pressures on $Pt/SiO_2/Si$ (1 0 0) wafers.

Oxygen pressure (mTorr)	Pb/(Pb + Sr)	Sr/(Pb + Sr)	Ti/(Pb + Sr)	O/(Pb + Sr)
50	0.55	0.45	0.86	2.41
80	0.57	0.43	0.93	2.59
100	0.52	0.48	1.12	3.00
200	0.53	0.47	1.39	3.69

where R is the resistance of the film and T_m is the measurement temperature. The phenomenon of strong NTCR, the values of resistance decrease with increasing T_m and biased fields, could be connected to the decrease in the resistance of semiconducting materials when the temperature increases. Figure 5(*c*) suggests that the bias field influences the temperature dependence of the film resistance, in particular at around $T_m = 200\,^{\circ}C$. In addition, the minimum of TCR shifts to lower T_m as the biased field increases.

Figure 6 shows the effect of oxygen pressure on the temperature dependence of R and the TCR properties from J–E data at $+75\,kV\,cm^{-1}$. The PLD PSrT films exhibit apparent NTCR behaviour, which is different from the bulk PSrT ceramics where a NTCR–PTCR transition is observed in the temperature range 123–390 °C [2–6]. The NTCR–PTCR transition can be explained on the basis of the conductivity. It is known that the conductivity is a product of carrier concentration and mobility terms. The NTCR–PTCR transition suggests a change in the mechanism of either one of the two contributions. It is reasonable to assume that the transition (NTCR to PTCR) is likely due to the transition from impurity ionization predominating at low temperatures to saturation at elevated temperatures where phonon scattering leads to a PTCR [25].

The mechanisms of PTCR and NTCR have been reported. To summarize, it has been suggested that the PTCR is attributed to the temperature-dependent barrier height and width at grain boundaries [26]. In Heywang's classical model for the PTCR in bulk ceramics, the PTCR behaviour is caused by trapped electrons at the grain boundaries. This model proposed that a double Schottky barrier is formed by capturing electrons at the grain boundaries. The barrier height increases with decreasing dielectric constant. The dielectric constant steeply decreases above the Curie point according to the Curie–Weiss law [27]. As a result, the carrier transport is hindered by increasing barrier height as the temperature increases and the PTCR behaviour is observed. On the other hand, the negative temperature effect of resistance is associated with the activation of electrons trapped by oxygen vacancies and the absence of grain boundaries [28]. As a result, the oxygen vacancies and grain boundaries may influence the TCR behaviour of the PSrT film.

It is noted that thin films usually do not exhibit a PTCR behaviour [29,30], because the grain sizes (50–300 nm) of thin films are much smaller than those of ceramic samples (several micrometres or larger). The ceramics are usually annealed at high temperatures (>1000 °C) and long time in order to get a large grain size and show the PTCR behaviour at low T_m. On the other hand, the grain size of the thin film is limited by its thickness. Therefore, except for some cases [31, 32], the PTCR behaviour is difficult to be observed in thin films. However, it is possible that the PTCR behaviour of PLD PSrT films appears only at temperatures above 390 °C, as reported by Chou *et al* in their work on PSrT bulk ceramics [6]. The evolution of temperature–resistance of PSrT films, which can estimate the Curie temperature (T_c) of PSrT by the electrical measurement, has been reported by Lu and Tseng [4] and Zhao *et al* [3]. It implies that the Curie temperature of PSrT films is higher than 390 °C and no phase transition of ferroelectric–paraelectric would occur at temperatures below 390 °C. In this study, due to the hardware limit, the maximum of T_m is 390 °C; hence, no ferroelectric–paraelectric transition is observed. Therefore, without phase transition, the effects of

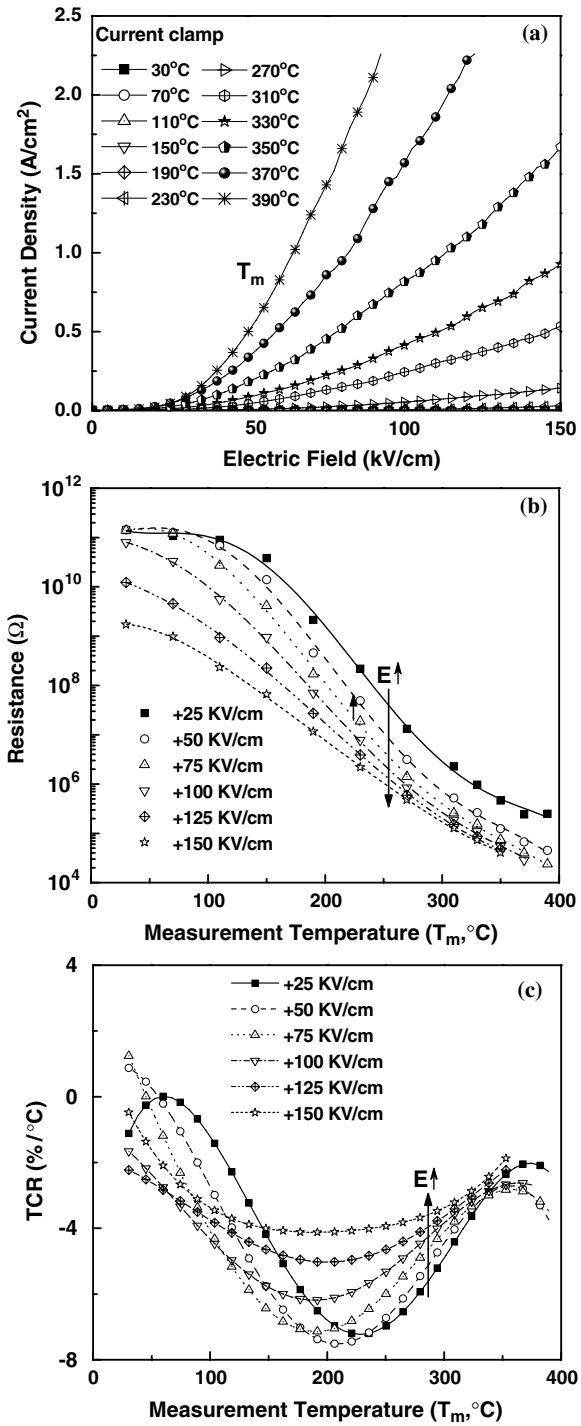

Figure 5. (*a*) Current density–electric field (*J*–*E*) curves, (*b*) resistance–temperature (*R*–*T*) curves and (*c*) TCR plots for Pt/PSrT/Pt capacitors prepared at 100 mTorr.

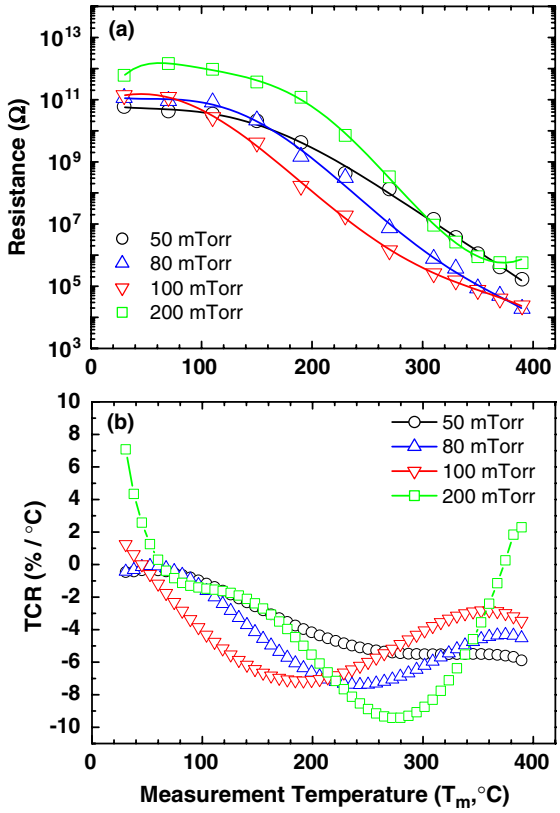

Figure 6. Resistance–temperature (*R*–*T*) curves and TCR plots (biased at +75 kV cm^{-1}) of Pt/PSrT/Pt capacitors prepared at various oxygen pressures.

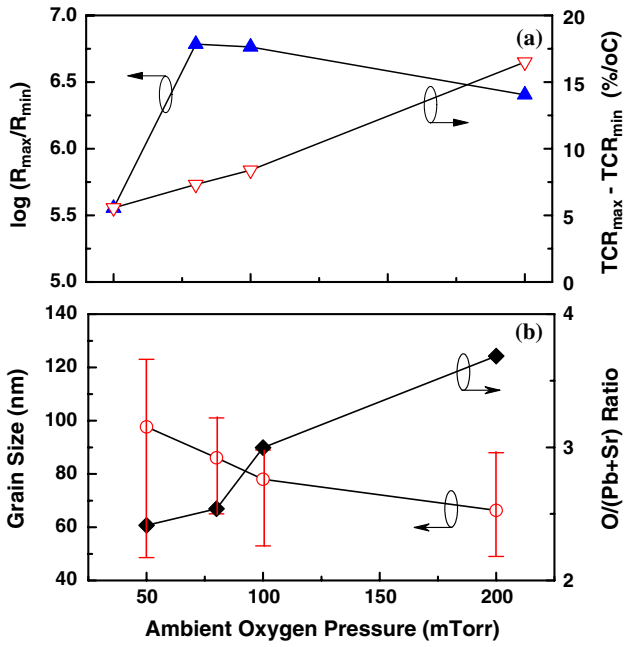

Figure 7. (*a*) log(R_{max}/R_{min}) and ($TCR_{max} - TCR_{min}$) and (*b*) grain size and O/(Pb + Sr) ratio of PSrT films deposited at various oxygen pressures.

oxygen pressure on resistance and NTCR could be attributed to material characteristics of films, originating from the changes in crystallinity, microstructure and composition (e.g. amorphous/crystalline phase, grain boundaries and oxygen vacancies). The connection between NTCR and material properties of PSrT films deposited at various oxygen pressures will be discussed later.

Figure 7(*a*) shows the resistance deviation log(R_{max}/R_{min}) and the TCR variation ($TCR_{max} - TCR_{min}$) as a function of the oxygen pressure, where R_{max} and R_{min} are the maximum and the minimum of film resistance, respectively, measured from 30 to 390 °C as given in figure 6(*a*). It is seen that the films deposited at 80 mTorr show the maximum resistance

Table 3. TCR characteristics of PSrT films in this work and PSrT bulk ceramics reported in the literature.

	This study	[2]	[3]	[4]	[5]	[6]
Materials	PSrT	PSrT	PSrT	Y-doped PSrT	Y-SiO_2-doped PsrT	Y-SiO_2-doped PsrT
Film/ceramic bulk	Film	Ceramic bulk	Ceramic bulk	Ceramic bulk	Ceramic bulk	Ceramic bulk
Preparation method	PLD	CS[b]	CS	CS	CS	CS of MS[c]
Electrode materials	Pt	In-Ga alloy	In-Ga alloy	In-Ga alloy	NA[a]	In-Ga alloy
Processing temperature (°C)	400	1100	950	1250	1080–1180	1150 or 1220
Measurement temperature (T_m, °C)	30–390	RT–400	RT–400	RT–500	RT–450	RT–700
Curie temperature (T_c, °C)	NA	150–200	123–212	140–280	165	CS : 210 MS : 390
NTCR or PTCR	Strong NTCR	NTCR–PTCR mixed	NTCR–PTCR mixed	NTCR–PTCR mixed	NTCR–PTCR mixed	NTCR–PTCR mixed
$\log(R_{max}/R_{min})$	NTCR : 5.55–6.78	NTCR : 0.45–1.38 PTCR : 4.85–5.25	NTCR : 0.11–1.86 PTCR : 3.23–4.50	NTCR : 0.7–1.5 PTCR : 3.6–5.0	NTCR : 2.7 PTCR : 4.7	NTCR : 1.0 PTCR : 2.5
$TCR_{max} - TCR_{min}$ (%/°C)	16.5	NA	NA	NA	10.2	NA

[a] Not available.
[b] Conventionally sintered.
[c] Microwave sintered.

deviation. Besides, TCR variation increases as the oxygen pressure increases. One can see that the PSrT film deposited at higher pressure has a larger TCR variation, indicating that it is more sensitive to the temperature change. Figure 7(*b*) shows the grain size and the O/(Pb + Sr) ratio of PSrT films deposited at various oxygen pressures. It suggests that the grain size (from SEM) decreases with increasing oxygen pressure, whereas the O/(Pb + Sr) ratio (table 2) increases with increasing oxygen pressure. It indicates that the TCR variation could be connected to the grain boundary density and the crystallized state of the films. The NTCR characteristic originates from the increase in the carrier charges when the temperature increases. The carrier charges in the conduction band may be thermally activated or detrapped from defect sites. Though the PSrT film deposited at a lower oxygen pressure contains more oxygen vacancies, it shows a weaker NTCR behaviour. The phenomenon may be attributed to the amorphous phase in the 50 mTorr-deposited PSrT film (figure 3(*a*)). The amorphous phase exhibits lower mobility than the crystalline phase. Therefore, the NTCR behaviour may be weakened by the reduced mobility of the PSrT film. Conversely, the PSrT film deposited at 200 mTorr shows a more dense and well-crystallized structure, which exhibits a stronger NTCR behaviour. On the other hand, the number of grain boundaries is increased with oxygen pressure. The grain boundary usually acts as a leakage current path of thin films. In addition, carrier generation at the grain boundary defects leads to additional leakage current. The dominant carrier generation mechanism at the grain boundary defects of insulating films is thermionic-field emission assisted by the temperature and the electric field [33]. As a result, for films with large grain boundary density, the current increases significantly when the temperature increases. Therefore, the NTCR behaviour is enhanced by increased grain boundaries.

Table 3 summarizes the Curie temperature, the resistance ratio and the TCR of PLD PSrT films in this study and the PSrT bulk ceramics reported in the literature. It is noticed that PLD PSrT films prepared at 400 °C exhibit strong NTCR behaviour with larger values of (R_{max}/R_{min}) than PSrT ceramics [2–6]. This result suggests that film-type PSrT is a better candidate for applications in miniaturized thermistor sensors due to its large resistance range in the temperature range of interest (30–390 °C).

4. Conclusions

In summary, the crystallinity and microstructure of PLD PSrT films are found to be dependent on the oxygen pressure. The ferroelectricity and paraelectricity of films are associated with the c/a ratio and the oxygen concentration. This result suggests that the ferroelectricity and paraelectricity of PSrT films could be realized by controlling the oxygen pressure during the PLD process. An NTCR behaviour of PSrT films is observed in the temperature range 100–390 °C. The PSrT film deposited at higher pressure reveals higher sensitivity to the temperature change. The large resistance deviation of the PLD PSrT film renders it a promising candidate as an embedded thermistor sensor in MEMS.

Acknowledgments

This work was supported by the National Science Council of ROC under the contract NSC95-2221-E-009-253. The authors would like to thank the Nano Facillity Center (NFC) in the National Chiao Tung University.

References

[1] Hamata Y, Takuchi H and Zomura K 1988 *Japanese Patent No* 63280401
[2] Zhao J, Li L and Gui Z 2002 *J. Eur. Ceram. Soc.* **22** 1171
[3] Zhao J, Li L, Qi J and Gui Z 2002 *J. Electroceram.* **9** 173
[4] Lu Y Y and Tseng T Y 1998 *Mater. Chem. Phys.* **53** 132
[5] Wang D J, Qiu J, Guo Y C, Gui Z L and Li L T 1999 *J. Mater. Res.* **14** 120
[6] Chou C C, Chang H Y, Lin I N, Shaw B J and Tan J T 1998 *Japan. J. Appl. Phys.* **37** 5269
[7] Shye D C, Chiou B S, Kuo M W, Chen J S, Bruce C S, Chou C, Jan K, Wu M F and Cheng H C 2003 *Electrochem. Solid State Lett.* **6** G55
[8] Horwitz J S, Chrisey D B, Dorsey P C, Knauss L A, Pond J M, Wilson M, Osofsky M S, Qadri S B, Caulfield J and Auyeung R C Y 1997 *Nucl. Instrum. Methods Phys. Res.* B **121** 371
[9] Karaki T and Adachi M 2005 *Japan. J. Appl. Phys.* **44** 692
[10] Nomura S and Sawada S 1955 *J. Phys. Soc. Japan* **10** 108
[11] Kang D H, Kim J H, Park J H and Yoon K H 2001 *Mater. Res. Bull.* **36** 265
[12] Zhang F, Karaki T and Adachi M 2005 *Japan. J. Appl. Phys.* **44** 6995
[13] Lim D G, Park Y, Moon S I and Yi J 2000 *Applications of Ferroelectrics 2000, ISAF 2000, Proc. 2000 12th IEEE Int. Symp. (Honolulu, 2000)* p 599
[14] Chrisey D B and Huber G K 1992 *Pulsed Laser Deposition of Thin Films* (New York: Wiley-Interscience) pp 55–87
[15] James A R and Prakash C 2004 *Appl. Phys. Lett.* **84** 1165
[16] Scarisoreanu N, Craciun F, Dinescu G, Verardi P and Dinescu M 2004 *Thin Solid Films* **453–454** 399
[17] Castro-Rodríguez R, Palomares-Sánchez S, Watts B E and Leccabue F 2003 *Mater. Lett.* **57** 3958
[18] Gao X S, Xue J M, Li J, Ong C K and Wang J 2003 *Microelectron. Eng.* **66** 926
[19] Chou C C, Hou C S, Chang G C and Cheng H F 1999 *Appl. Surf. Sci.* **142** 413
[20] Chou C C, Hou C S and Cheng H F 1998 *Ferroelectrics* **206–207** 393
[21] Hou C S, Pan H C, Chou C C and Cheng H F 1999 *Ferroelectrics* **232** 129
[22] Wang D N, Hovmöller S, Kihlborg L and Sundberg M 1988 *Ultramicroscopy* **25** 303
[23] Li C L, Chen Z H, Zhou Y L and Cui1 D F 2001 *J. Phys.: Condens. Matter* **13** 5361
[24] Fuchs D, Adam M, Schweiss P, Gerhold S, Schuppler S, Schneider R and Obst B 2000 *J. Appl. Phys.* **88** 1844
[25] Kim I-D, Rothschild A and Tuller H L 2006 *Appl. Phys. Lett.* **88** 072902
[26] Heywang W 1961 *Solid-State Electron.* **3** 51
[27] Kittel C 1996 *Introduction to Solid State Physics* 7th edn (New York: Wiley)
[28] Han W H, Chen X K, Xie E Q, Wu G, Yang J P, Wang R, Cao S Z and Wang Y L 2007 *Surf. Coat. Technol.* **201** 5680
[29] Lemee N, Dubourdieu C, Delabouglise G, Senateur J P and Laroudie F 2002 *J. Cryst. Growth* **235** 347
[30] Panda B, Roy A, Dhar A and Ray S K 2007 *J. Appl. Phys.* **101** 064116
[31] Okano M, Watanabe Y and Cheong S-W 2003 *Appl. Phys. Lett.* **82** 1923
[32] Hwang C S, Lee B T, Cho H J, Lee K H, Kang C S, Horii H, Lee S I and Lee M Y 1997 *Appl. Phys. Lett.* **71** 371
[33] Sze S M 1985 *Physics of Semiconductor Devices* 2nd edn (New York: Wiley)